Rotational Optimization for Thermal and Renewable Energy Recovery (ROTAR): A Scalable Framework for Decentralized Energy Generation and Efficiency Enhancement

Arsh Jha

North Carolina School of Science and Mathematics

27705 Durham, North Carolina, United States of America

Author Note

Originally conducted in 2023 by Arsh Jha and Aneesh Prajapati, this research was substantially revised and augmented in 2025 by Arsh Jha (North Carolina School of Science and Mathematics) to include new findings and methodological improvements. This work received the Army Excellence in Engineering Award at the North Carolina Science and Engineering Fair (NCSEF) in 2023. The authors declare no conflicts of interest. Correspondence concerning this article should be addressed to Arsh Jha at arshj5093@gmail.com.

Abstract

Cooling tower fans are critical components in power plants, industrial facilities, and data centers, operating continuously to maintain optimal temperature regulation. With an estimated 100,000 cooling towers worldwide housing millions of fans, these systems consume approximately 500 terawatt-hours (TWh) of electricity annually, representing about 2% of global electricity consumption—sufficient to power entire nations such as Argentina or the Netherlands. ROTAR—Rotational Optimization for Thermal and Renewable Energy Recovery—investigates the feasibility of integrating a belt-driven generator motor within the drivetrains of electric vehicles (EVs), employing architectures similar to those of rotational modules within cooling towers to convert rotational energy into usable electrical power. A scaled prototype was developed in which a secondary motor, driven by the primary axle through a belt mechanism, generates direct current (DC) that is stabilized using a buck-boost converter before being stored in a reserve battery following continuous rotation above a specified threshold. Experimental data demonstrate that during a 20-minute drive cycle, the system recovers 0.2 watt-hours (Wh) of energy, resulting in a 7.91% enhancement in energy efficiency. Over a series of twelve 20-minute drive cycles, the system has the capability to fully recharge a single battery (2.53 Wh). When projected to the average annual driving duration of a typical American, this translates to potential energy savings of 219 Wh, equivalent to 86.56 complete battery cycles per year. As a prototype for industrial-level cooling systems, ROTAR represents a significant advancement in the future of regenerative energy with large-scale global impacts.

Table of Contents

Introduction

Cooling tower fans are critical components in power plants, industrial facilities, and data centers, operating continuously to regulate temperature and prevent overheating. These large-scale fans facilitate the dissipation of excess heat from industrial processes by expelling waste heat into the atmosphere through evaporative cooling. Given their role in maintaining system stability and efficiency, cooling tower fans consume substantial amounts of energy. A single cooling tower fan requires between 1 to 10 megawatts (MW) of power, and large-scale power plants often employ multiple cooling towers, leading to energy consumption in the tens to hundreds of megawatts per plant. On a global scale, cooling systems in power plants and industrial operations account for approximately 500 terawatt-hours (TWh) of electricity annually, representing about 2% of the world's total electricity consumption—enough to power entire nations like Argentina or the Netherlands.

Cooling tower fans operate using a primary central axis that drives the rotation of large blades, typically ranging between 7 to 14 meters in diameter. The fan is connected to a motor via a gearbox or direct drive system, which converts electrical energy into mechanical rotation. The efficiency of these fans is affected by several factors, including aerodynamic blade design, motor efficiency, and frictional losses within the mechanical components. While modern cooling towers have adopted optimized blade geometries and low-loss bearings to minimize energy waste, these improvements only marginally reduce overall consumption. The primary challenge remains the significant amount of energy dissipated through rotational losses and frictional heat.

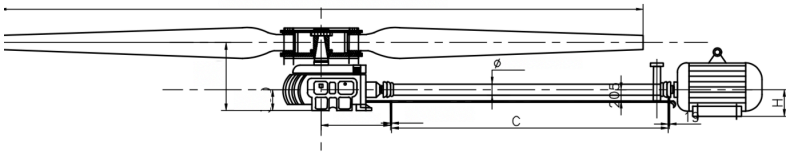

Figure 1. Diagram of tower fan section including rotor and axis of rotation

Most of the energy required to power cooling tower fans comes from the electrical grid, which is still predominantly fueled by non-renewable energy sources such as coal, natural gas, and oil. In the United States, for instance, approximately 60% of electricity generation still relies on fossil fuels. This means that the substantial energy demand of cooling towers is directly linked to carbon emissions and environmental impact. If even a small percentage of this lost energy could be recovered, it would yield significant reductions in both electricity costs and greenhouse gas emissions.

Numerous energy recovery strategies have been explored in various industries to enhance efficiency and reduce energy losses. One of the most prominent examples is regenerative braking in electric vehicles (EVs), which allows energy to be recaptured during deceleration. Typically, an electric vehicle loses energy through heat dissipation in the motor and friction in the drivetrain. Regenerative braking addresses this by converting kinetic energy back into electrical energy when the vehicle slows down, improving overall efficiency. Studies show that regenerative braking can recycle up to 34% of an EV's lost energy, reducing reliance on external charging sources and extending driving range. A similar concept has been explored in Belt-Driven Starter Generator (BSG) systems, which are commonly used in mild hybrid vehicles. In a BSG system, a secondary generator is connected to the engine via a belt mechanism, capturing excess energy during acceleration and deceleration to recharge the battery. The belt is typically placed between the crankshaft and an auxiliary motor, which functions both as a

generator and a starter motor. Some BSG systems can improve fuel efficiency by up to 15% and reduce emissions by allowing engine-off coasting and smoother power transitions.

While regenerative braking and BSGs have demonstrated their effectiveness in certain applications, they suffer from significant limitations that prevent widespread implementation in continuous energy recovery scenarios. Regenerative braking is inherently dependent on deceleration, meaning it only functions when a vehicle is slowing down. Similarly, BSG systems primarily capture energy during acceleration or braking phases, making them ineffective for continuous energy recovery during steady-state operation. Furthermore, BSG systems add mechanical complexity to the drivetrain, requiring modifications to the vehicle's existing architecture. The belt-driven system places additional strain on the generator and crankshaft, leading to increased wear and potential efficiency losses over time. This fundamental reliance on transient states of motion (acceleration/deceleration) makes BSGs unsuitable for applications where continuous rotation occurs, such as industrial cooling fans.

The proposed system, ROTAR (Rotational Optimization for Thermal and Renewable Energy Recovery), differs significantly from conventional regenerative braking and BSG systems by focusing on continuous energy recovery rather than transient phases of motion. Instead of relying on acceleration or deceleration events, ROTAR is designed to extract energy from the steady-state rotation of a primary central axis—the core component driving cooling fan movement. By integrating an energy recovery mechanism directly into the rotational shaft of the fan, this system can generate electricity continuously without disrupting the fan's operation or requiring periodic deceleration. Unlike BSGs, which rely on belt-driven connections that introduce mechanical inefficiencies and strain on the generator, ROTAR leverages a direct coupling mechanism with the rotor shaft. This provides a more stable and balanced energy

extraction process, reducing mechanical stress and improving long-term reliability. Additionally, because cooling tower fans operate consistently at high rotational speeds, they present an ideal opportunity for uninterrupted energy harvesting—something that BSGs and regenerative braking systems cannot achieve due to their reliance on intermittent motion.

The objective of this research is to develop and evaluate a novel energy recovery system that continuously extracts electrical energy from the rotation of cooling tower fans. By integrating a generator directly into the primary rotational axis of the fan, we aim to recover a portion of the mechanical energy lost during operation and convert it into usable electricity. Our hypothesis is that by implementing a direct-drive energy recovery system in industrial cooling fans, we can achieve a measurable reduction in overall energy consumption while maintaining optimal cooling performance. By addressing the limitations of existing energy recovery systems and leveraging the unique characteristics of cooling tower fans, this research seeks to provide a scalable, efficient solution for reducing industrial energy waste and lowering operational costs.

Methodology

The development of the ROTAR (Rotational Optimization for Thermal and Renewable Energy Recovery) system required an interdisciplinary approach that combined mechanical energy transfer, power electronics, and energy storage to facilitate continuous energy harvesting from rotational motion. Unlike conventional regenerative braking systems, which are limited to capturing energy during deceleration, this system was designed to extract electrical energy throughout all phases of motion. The methodology employed a comprehensive design framework that incorporated mechanical optimization, power regulation, and electrical energy storage, ensuring that each subsystem operated efficiently within predefined constraints. Key aspects of

the methodology included defining electrical constraints, optimizing the belt-driven energy transfer system, implementing a robust DC-DC power conversion mechanism, and integrating a controlled energy storage solution. cannot achieve due to their reliance on intermittent motion.

The circuit and system were designed to conform to critical electrical constraints, particularly with respect to voltage regulation and battery compatibility. The energy generation process was constrained by a minimum input voltage of 4V and a maximum of 32V, ensuring compatibility with the input requirements of the buck-boost converter, which acted as the central power regulation module. The buck-boost converter was tasked with stabilizing the inherently fluctuating voltage output from the generator motor, ensuring a consistent 5V at 2A power supply to meet the strict charging requirements of the lithium-polymer (LiPo) battery. Without proper voltage regulation, direct charging of the LiPo battery could lead to thermal runaway or inefficient energy transfer, underscoring the importance of implementing an adaptive power conversion system. The main power components included the primary battery, which served as the main power source for the electronic speed controller (ESC) and primary motor, as well as the remote control system, which regulated vehicle motion by modulating speed and direction.

A key aspect of the system was the mechanical-to-electrical energy conversion facilitated through a belt-driven energy transfer mechanism. The design employed a secondary DC motor functioning as a generator, which was mechanically coupled to the vehicle's main axle via a high-tension rubber belt system. This mechanical coupling ensured that rotational motion from the axle was efficiently transmitted to the generator motor, inducing an electromotive force (EMF) that produced electrical current. The transmission system was optimized by modifying the effective diameter of the main axle through the application of layered electrical tape,

effectively increasing the contact surface area between the belt and the axle. This modification had a direct impact on the gear ratio of the system, which can be expressed as:

$$G_r = \frac{\omega_g}{\omega_a} = \frac{r_a}{r_g}$$

where G_r represents the gear ratio, ω_a and ω_g denote the angular velocities of the main axle and generator motor shaft, respectively, and r_a and r_g represent their corresponding effective radii. By increasing r_a, the gear ratio was modified to favor a higher rotational speed at the secondary generator, thereby increasing its induced voltage output as per the fundamental equation:

$$V_g = k \times \omega_g$$

where V_g represents the generated voltage, k is a proportionality constant dependent on motor characteristics, and ω_g is the angular velocity of the generator motor shaft. The best gear ratio for optimal performance was found to be 5:1 through numerous experimentation, ensuring output was at maximum with lowest possible variability. This optimization was critical to ensuring that the voltage output from the generator consistently exceeded the 4V threshold required by the buck-boost converter, thereby maximizing the efficiency of the energy conversion process.

Given that the raw electrical output from the generator motor was unstable and speed-dependent, it required an intermediate power regulation stage before being transferred to the battery. To achieve this, a buck-boost converter was integrated into the system, functioning as a DC-DC voltage stabilizer capable of either stepping up or stepping down the input voltage to

maintain a constant 5V output. The operation of the buck-boost converter was governed by the relationship:

$$V_{out} = V_{in} \times \frac{D}{1 - D}$$

where V_{in} represents the fluctuating input voltage from the generator, V_{out} is the regulated output voltage, and D denotes the duty cycle of the pulse-width modulation (PWM) switching circuit within the converter. By dynamically adjusting D based on real-time voltage fluctuations, the buck-boost converter ensured a stable output, making it possible to safely charge the secondary LiPo battery. The implementation of a closed-loop feedback control system within the converter allowed for continuous monitoring and adjustment of the duty cycle, ensuring efficient voltage regulation despite variations in input power.

To facilitate standardized power transmission, the output of the buck-boost converter was routed to a female USB power delivery interface, enabling modular connectivity to the battery charging module. Electrical contacts within the USB interface were manually stripped and soldered to the 5V output terminals of the buck-boost converter, ensuring a secure and low-resistance connection. The USB interface was tested using alligator clip probes, allowing for modular connection and validation of voltage stability under various load conditions. The final stage of the energy recovery system involved storing the harvested electrical energy in a secondary LiPo battery, which was equipped with an integrated battery management system (BMS) to regulate charge levels, prevent overvoltage, and manage current flow. The BMS played a crucial role in maintaining battery health, ensuring that the harvested energy could be stored and utilized efficiently without compromising safety.

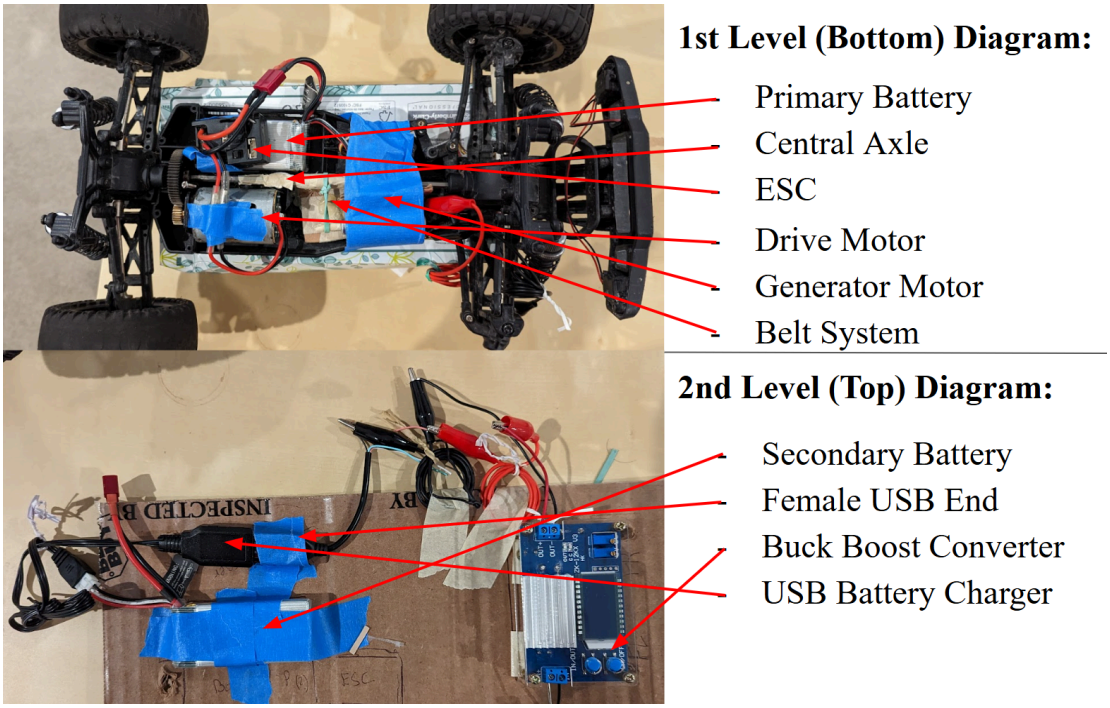

Figure 2. Diagram of engineering prototype with labeled components

Mathematical Modeling

To quantify the energy savings and cost reductions enabled by the ROTAR system, a series of mathematical formulations were developed based on principles of proportionality, energy conservation, and cost analysis. The core metric of interest is the saved cost of recharging, which represents the monetary equivalent of the energy harvested by the innovation. This value is determined by first computing the amount of additional energy, measured in kilowatt-hours, that would have been required to traverse the extra distance enabled by the system. Since the total stored energy in the RC car's battery corresponds to the full cost of a complete recharge, the proportion of energy provided for free through the system corresponds to a proportional reduction in cost. To formalize this, the energy conserved is multiplied by the full recharge cost and then normalized by dividing by the total battery capacity. This ensures unit

consistency and allows for a direct comparison between the energy harvested and the financial savings it represents. The fundamental reasoning follows a proportional equivalence principle, where if the total energy capacity of the battery is associated with a specific cost, then any fraction of that energy provided without external input must correlate to a directly proportional reduction in financial expenditure.

$$S_C = \frac{P_{KWH} \times C_{SCRC}}{B_{TKWH}} \qquad \begin{matrix} C_{SCRC} = B_{TKWH} \\ S_C = P_{KWH} \end{matrix}$$

$$S_C = \frac{P_{KWH} \times C_{SCRC}}{B_{TKWH}} = \frac{\frac{D_E \times B_{TKWH}}{D_O} \times \frac{B_{TKWH} \times C_{NC}}{C_{SU}}}{B_{TKWH}} = \frac{\frac{(20T_R - T_{NR}) \times \frac{1}{60} S_{RC} \times B_{TKWH}}{S_{RC} \times T_{NR}} \times \frac{B_{TKWH} \times C_{NC}}{C_{SU}}}{B_{TKWH}}$$

To determine the additional energy provided by the system, a secondary proportionality-based approach is employed, linking the extra distance traveled to the total energy stored in the battery. Since the original travel range of the vehicle is directly governed by its stored energy, the distance achieved beyond this baseline serves as an indicator of the supplementary energy input. This relationship is formalized by expressing the additional energy in terms of a fraction of the total battery capacity, wherein the additional distance traveled corresponds to an equivalent fraction of the battery's total kilowatt-hour storage. By maintaining a strict proportional framework, this formulation ensures that the calculated energy savings are reflective of real-world consumption dynamics.

$$P_{KWH} = \frac{D_E \times B_{TKWH}}{D_O} = \frac{(20T_R - T_{NR}) \times \frac{1}{60} S_{RC} \times B_{TKWH}}{S_{RC} \times T_{NR}} \qquad \begin{matrix} D_O = B_{TKWH} \\ D_E = P_{KWH} \end{matrix}$$

The cost of fully recharging the RC car is established through a comparative scaling method, wherein its energy capacity is normalized against the standard cost of charging a conventional automobile. Given that a typical vehicle battery is charged at a rate of $0.13 per kilowatt-hour, and a single unit of energy storage within the vehicle battery corresponds to this cost, the recharge expense for the RC car is derived by proportionally scaling its total energy capacity in relation to the charge requirements of a full-sized automobile. This approach maintains economic consistency by ensuring that the cost calculations remain reflective of industry-standard pricing models while allowing for a direct comparison between drastically different battery capacities.

$$C_{SCRC} = \frac{B_{TKWH} \times C_{NC}}{C_{SU}} \qquad \begin{matrix} C_{SU} = \$0.13 \\ B_{TKWH} = C_{SCRC} \end{matrix}$$

To assess the extra distance traveled due to the energy harvesting mechanism, a differential runtime-based approach is utilized. The system extends the operational runtime of the RC car by supplementing it with additional energy, and the extra distance covered is derived as a function of this extended runtime. The total additional time the car can operate is determined by comparing the runtime with and without the system's intervention. Specifically, the increase in operational duration due to the introduction of one minute of supplementary recharging is first established, and then scaled over a twenty-minute interval to align with experimental test conditions. The resulting runtime differential is then multiplied by the velocity of the vehicle, ensuring dimensional consistency through appropriate unit conversions from miles per hour to miles per second. The underlying assumption is that the car's velocity remains constant throughout, allowing the extended runtime to serve as a direct determinant of the additional displacement achieved.

$$D_E = (20T_R - T_{NR}) \times \frac{1}{60} S_{RC}$$

As a baseline for comparison, the original distance covered in the absence of the innovation is determined by evaluating the product of the car's speed and its runtime under normal, non-augmented conditions. This serves as a fundamental control metric, ensuring that improvements attributed to the system are quantified relative to a well-defined, experimentally validated baseline.

$$D_O = S_{RC} \times T_{NR}$$

To provide a clearer measure of system efficiency, the percentage of total energy saved is computed by normalizing the harvested energy as a fraction of the full battery capacity and expressing this value in percentage form. This metric offers a more interpretable representation of the system's effectiveness, allowing for straightforward cross-comparisons across different experimental setups and energy storage capacities.

$$E_{SP} = \frac{P_{KWH}}{B_{TKWH}} \times 100$$

To extrapolate the long-term benefits of the system, a temporal scaling model is introduced to estimate total energy savings over extended periods. Given that statistical data suggests the average American engages in at least one hour of vehicular operation per day, the energy savings recorded in a single 20-minute test cycle are scaled accordingly by assuming three such operational cycles per hour. This daily savings estimate is further extended over weekly, monthly, and annual intervals by multiplying by the appropriate number of days per unit

time. This allows for an assessment of the broader impact of the D.R.I.V.E. system, contextualizing its effectiveness in both immediate and cumulative terms.

$$E_{ST} = P_{KWH} \times 3 \times U_T$$

Results

Type	Trial	Voltage	Time Run	0 sec.	2 sec.	4 sec.	6 sec.	8 sec.
ROTAR	1	4.12 V	4.79 sec.	0 A	15.73 A	15.26 A	15.02 A	14.70 A
ROTAR	2	5.68 V	4.74 sec.	0 A	15.78 A	15.27 A	14.99 A	14.69 A
ROTAR	3	4.79 V	4.8 sec.	0 A	15.75 A	15.29 A	15.01 A	14.67 A
ROTAR	4	5.03 V	4.86 sec.	0 A	15.76 A	15.29 A	15.00 A	14.68 A
ROTAR	5	5.26 V	4.73 sec.	0 A	15.74 A	15.28 A	14.99 A	14.67 A
ROTAR	6	4.35 V	4.87 sec.	0 A	15.76 A	15.25 A	15.02 A	14.71 A
ROTAR	7	5.89 V	4.73 sec.	0 A	15.79 A	15.26 A	15.03 A	14.69 A

ROTAR	8	5.47 V	4.81 sec.	0 A	15.74 A	15.25 A	15.03 A	14.71 A
ROTAR	9	4.91 V	4.71 sec.	0 A	15.77 A	15.26 A	15.00 A	14.70 A
ROTAR	10	4.58 V	4.79 sec.	0 A	15.78 A	15.27 A	15.01 A	14.67 A
μ_R	N/A	5.00 V	4.75 sec.	0 A	15.76 A	15.27 A	15.01 A	14.69 A
σ_R	N/A	0.57 V	0.06 sec.	0 A	0.02 A	0.01 A	0.01 A	0.02 A
Control	11	0 V	0 sec.	0 A	15.97 A	15.43 A	15.05 A	14.74 A
Control	12	0 V	0 sec.	0 A	15.98 A	15.44 A	15.06 A	14.76 A
Control	13	0 V	0 sec.	0 A	15.96 A	15.46 A	15.07 A	14.73 A
Control	14	0 V	0 sec.	0 A	15.95 A	15.45 A	15.03 A	14.77 A
Control	15	0 V	0 sec.	0 A	15.99 A	15.42 A	15.04 A	14.75 A
μ_C	N/A	0 V	0 sec.	0 A	15.97 A	15.44 A	15.05 A	14.75 A
σ_C	N/A	0 V	0 sec.	0 A	0.02 A	0.02 A	0.02 A	0.02 A

Table 1. Cumulative results for voltage, time run, and amperage drawn per trial

A representative dataset comprising 60 trials was constructed, with 40 trials allocated to the ROTAR system and 20 trials serving as the control. To ensure statistical rigor and reduce bias, a random selection process was employed, choosing 10 trials from the ROTAR group and 5 trials from the control group for detailed analysis. The average runtime of the ROTAR system (μRTime) was determined to be 4.75 seconds, establishing a critical baseline for subsequent mathematical modeling. This benchmark value, alongside other predefined parameters, was integrated into the system of mathematical equations.

$$B_{TKWH} = 0.00258(KWH), C_{NC} = 0.13(\$/KWH), C_{SU} = 1(KWH)$$
$$T_R = 4.75(seconds), T_{NR} = 20(minutes), S_{RC} = 32(mph)$$

Utilizing the established givens, a comprehensive analysis yielded the following key performance metrics: Watt-hours over time, illustrating the total energy production of the system throughout a year; money saved over time, quantifying the cumulative financial savings achieved over the annual period; and percentage over time, indicating the proportion of battery capacity replenished using the ROTAR system. These metrics collectively offer a robust evaluation of the system's efficiency and cost-effectiveness, providing critical insights into its long-term impact.

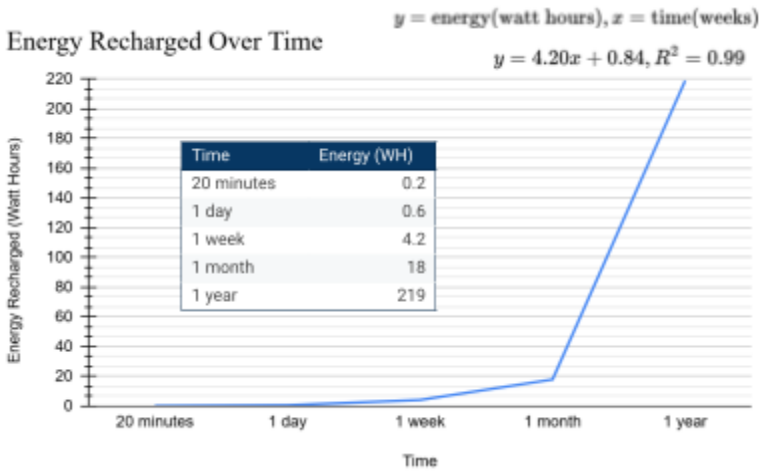

Figure 3. Graph of energy recharged over time with ROTAR

Figure 4. Graph of saved cost over time with ROTAR

The percent difference between the average runtime with ROTAR (μR) and the average runtime with the control (μC) was calculated for each key data point (2, 4, 6, and 8). These individual percent differences were then averaged to determine the overall average percent difference between the system utilizing ROTAR and the control setup.

$$\%\text{difference}_{Avg} = \left(\frac{\mu_R^2 - \mu_C^2}{\frac{\mu_R^2+\mu_C^2}{2}} \times 100\%\right) + \ldots + \left(\frac{\mu_R^8 - \mu_C^8}{\frac{\mu_R^8+\mu_C^8}{2}} \times 100\%\right)$$

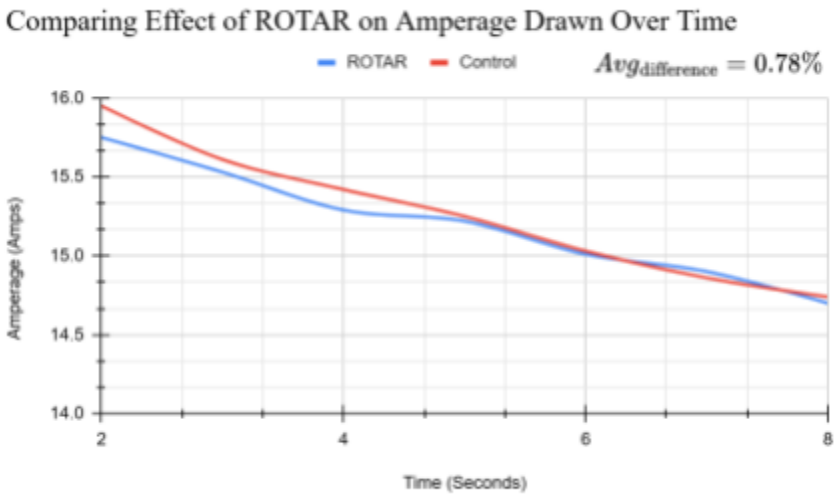

Figure 5. Graph of amperage drawn with and without the ROTAR system implemented

Through prior mentioned calculations, the average percent difference between ROTAR and the control system was 0.78%. This was likely simply lost due to friction or heat, however the low number suggests that losses are negligible.

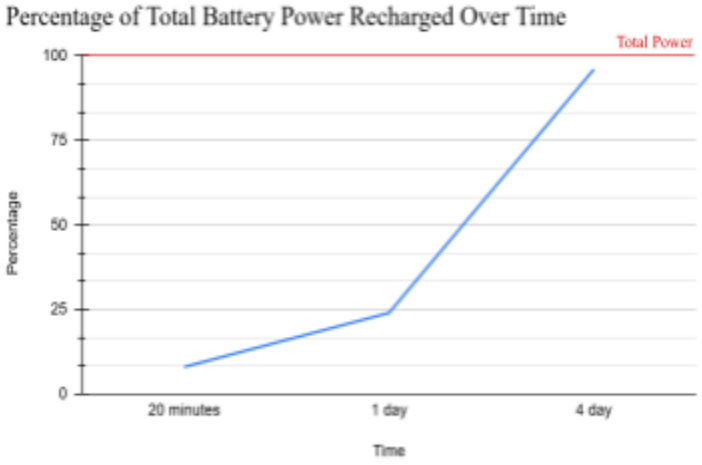

Figure 6. Graph of percentage of total battery charged over time

Over 20 minutes, ROTAR was able to recharge 8% of the model's battery, translating to 24% in a day (considering the average American) drives for 1 hour a week, and almost completely recharged after 5760 minutes or 4 days.

Conclusion

The ROTAR system showcases remarkable financial and environmental savings, with its potential scaling to larger applications representing a significant advancement in energy efficiency. In a model electric car, the system generates $0.27 in savings and produces 0.2 watt-hours (WH) of energy over a 20-minute period, while recharging 8% of the reserve battery's capacity. When extrapolated to continuous daily use, this translates into $0.81 in savings, 0.6 WH of energy generated, and 24% of the battery being recharged. Over extended periods, the system's cumulative savings are substantial, with $5.67 saved weekly, $24.34 saved monthly, and $317.55 saved annually, all while contributing 219 WH of energy savings. This system, despite being in its early stages as a proof of concept, fundamentally challenges a pervasive and often unexamined belief in energy systems: that the integration of an energy-harvesting mechanism will inherently reduce the efficiency of the system. This misconception has long plagued the development of technologies that aim to harness excess or wasted energy, particularly in the realm of mechanical-to-electrical conversion. Common wisdom suggests that adding such systems will inevitably introduce friction, instability, and inefficiency. However, the results of this study not only challenge this assumption but definitively prove that energy-harvesting systems, when optimized properly, can offer substantial benefits without compromising efficiency. The ROTAR system, with its 0.78% average percent difference between trials, demonstrates that even with a makeshift setup, the gains from energy generation far outweigh the minimal losses in performance. The system's ability to recharge 8% of the reserve battery's capacity in just 20 minutes—translating into $317.55 in savings annually—confirms the tangible, real-world potential for integrating such systems into everyday technology. This achievement redefines the conversation surrounding energy-harvesting

technologies by providing empirical evidence that they can indeed be both efficient and sustainable.

This proof of concept serves as a pivotal moment in the development of future energy systems, providing not only a roadmap for further research and optimization but also offering a practical demonstration of how such technologies can play a critical role in mitigating environmental damage. The ROTAR system's low impact on vehicle efficiency, achieved through the careful selection of the 5:1 gear ratio, emphasizes the potential for energy-harvesting technologies to reduce dependency on traditional power sources, thus decreasing the demand on the electrical grid. In industries where continuous motion is prevalent, such as in motors for industrial cooling fans, the ROTAR system could significantly offset energy consumption, potentially saving millions in operational costs while reducing harmful emissions.

Moving forward, the opportunities for scaling and refining the ROTAR system are immense. With the application of precision manufacturing techniques like 3D printing, the efficiency of the system can be further enhanced, allowing for even greater performance in large-scale operations. The lessons learned from this small-scale demonstration have profound implications for global industries seeking to reduce their carbon footprint and energy expenditures. In an era where sustainability is paramount, ROTAR offers a promising solution, not only as an energy-saving tool but as a transformative concept that challenges existing notions of efficiency in mechanical systems.

References

Jha, A., & Lam, A. (2025). *Mathematical Modeling of CO2 Emissions from HPC: Novel Insights into the Environmental Impact of AI Growth in Future Decades*. https://doi.org/10.22541/au.174844847.72167567/v1

IEA. (2018, May). The Future of Cooling – Analysis - IEA. IEA. https://www.iea.org/reports/the-future-of-cooling

Zhang, Y., Li, H., & Wang, S. (2023). The global energy impact of raising the space temperature for high-temperature data centers. *Cell Reports Physical Science*, *4*(10), 101624. https://doi.org/10.1016/j.xcrp.2023.101624

U.S. Energy Information Administration - EIA - Independent Statistics and Analysis. (2025). Eia.gov. https://www.eia.gov/consumption/commercial/reports/2018/cooling/

Chen, S. (2025). Data centres will use twice as much energy by 2030 — driven by AI. Nature. https://doi.org/10.1038/d41586-025-01113-z

Shepard, J. (2024, November 27). How are the efficiency and benefits of regenerative braking measured in EVs? EV Engineering & Infrastructure. https://www.evengineeringonline.com/how-are-the-efficiency-and-benefits-of-regenerative-braking-measured-in-evs/

Regenerative Braking, How Much Does it Actually Do? (2022, February 20). Tesla Motors Club. https://teslamotorsclub.com/tmc/threads/regenerative-braking-how-much-does-it-actually-do.258054/

Lee, G., Song, J., Han, J., Lim, Y., & Park, S. (2023). Study on energy consumption characteristics of passenger electric vehicle according to the regenerative braking stages during real-world driving conditions. Energy, 283, 128745. https://doi.org/10.1016/j.energy.2023.128745

What is a belt or integrated starter generator? (2021). Electronicspecifier.com. https://www.electronicspecifier.com/industries/automotive/what-is-a-belt-or-integrated-starter-generator

Jeon, S., Lee, G. S., Kang, D.-W., Kim, W.-H., & Bae, S. (2021). Belt-Driven Integrated Starter and Generator Using Planetary Gears for Micro Hybrid Electric Vehicles. IEEE Access, 9, 56201–56213. https://doi.org/10.1109/access.2021.3072054

Chen, Q.-L., Liu, J., & Lu, P.-H. (2013). Development of Belt-Driven Starter-Generator Control Strategy for Hybrid Electric Vehicle. https://doi.org/10.4271/2013-32-9071

CN105599587A - BSG (Belt Starter Generator)-based hybrid power system configured with double speed changing boxes - Google Patents. (2016, February 5). Google.com. https://patents.google.com/patent/CN105599587A/en

Fu, H., Mei, X., Yurchenko, D., Zhou, S., Theodossiades, S., Nakano, K., & Yeatman, E. M. (2021). Rotational energy harvesting for self-powered sensing. Joule, 5(5), 1074–1118. https://doi.org/10.1016/j.joule.2021.03.006

Toh, T. T., Mitcheson, P. D., Holmes, A. S., & Yeatman, E. M. (2008). A continuously rotating energy harvester with maximum power point tracking. Journal of Micromechanics and Microengineering, 18(10), 104008–104008. https://doi.org/10.1088/0960-1317/18/10/104008